

## **BRIGHT AND DARK SOLITON GENERATION IN A LEFT-HANDED NONLINEAR TRANSMISSION LINE WITH SERIES NONLINEAR CAPACITORS**

**F. G. Gharakhili**

School of Electrical and Computer Engineering  
University of Tarbiat Modares  
Tehran, Iran

**M. Shahabadi**

School of Electrical and Computer Engineering  
University of Tehran  
Tehran, Iran

**M. Hakkak**

School of Electrical and Computer Engineering  
University of Tarbiat Modares  
Tehran, Iran

**Abstract**—In this article, we demonstrate that in the case of a positive group velocity left-handed nonlinear (LH-NL) transmission line with *series* nonlinear capacitances, the spatial derivative of the voltage distribution satisfies the nonlinear Schrödinger (NLS) equation. Consequently, it will shown that a LH-NL transmission line with series varactors can be used to generate both bright and dark solitons similar to a composite right-left-handed (CRLH) transmission line periodically loaded with *shunt* varactors. The paper also discusses the conditions for generation of bright and dark solitons.

### **1. INTRODUCTION**

Left-handed (LH) metamaterials with simultaneously negative permeability and permittivity have attracted the attention of microwave and RF engineers in recent years [1–6]. First, Veselago investigated electromagnetic properties of these materials theoretically in 1968 [7]. He

---

Corresponding author: F. G. Gharakhili (geran\_e@yahoo.com).

predicted that LH metamaterials exhibit negative refractive index [7, 8] that leads to reversal of Snell's law, of the Doppler effect, and of the Cherenkov radiation. At the microwave frequencies, a number of transmission line with LH characteristics have been proposed so far [9–11]. Furthermore, because of their anomalous dispersion, the LH transmission lines can support soliton waves when they are properly loaded with nonlinear components [12]. In [13], Caloz introduces a balanced CRLH transmission line with shunt voltage-dependent capacitors and demonstrates that both bright and dark solitons can propagate on the proposed transmission line. A comparable realization to [13] can be found in [14] where a reductive perturbation method [15] is used to analyze soliton generation. Another implementation of a LH-NL transmission line is introduced in [16]. There, a pump signal is applied to a LH-NL transmission line excites both bright and dark solitons. The reader is referred to [17] which summarizes most of the recent research on the LH-NL transmission line. In [18], the soliton propagation on LH anharmonic chains with negative group velocity is investigated by the quasi-continuum approach, where it is shown that small-amplitude solitons can propagate for any value of wave number in the first Brillouin zone.

In this paper, we proposed a LH-NL transmission line periodically loaded with *series* nonlinear capacitances and linear shunt inductances. For the proposed transmission line, we will demonstrate generation of both bright and dark solitons. In Section 2, the governing wave equation for this LH-NL transmission line is obtained. In Section 3, a *reductive perturbation method* is applied to the proposed LH-NL transmission line and a closed-form solution is presented. Simulation results for verification of the obtained solution are given in Section 4. Finally, Section 5 discusses the generation of soliton based on the results obtained in the previous sections.

## 2. FORMULATION OF A LH-NL TRANSMISSION LINE WITH SERIES VARACTORS

A circuit model of a LH-NL transmission line with  $N$  identical cells is given in Fig. 1. Each cell of the model under consideration is contains a series varactor diodes and a linear shunt inductance. Here,  $V_n$  and  $u_n = V_n - V_{n+1}$  are the voltage of the  $n$ th node and the voltage across the  $n$ th varactor, respectively. In this paper, we have neglected the dissipation of the LH-NL transmission line. Also in [18], the case in which the shunt inductors are nonlinear but the series capacitors are linear is also studied, although the implementation of capacitors seem to be more practical.

The LH-NL transmission line shows two effects simultaneously.

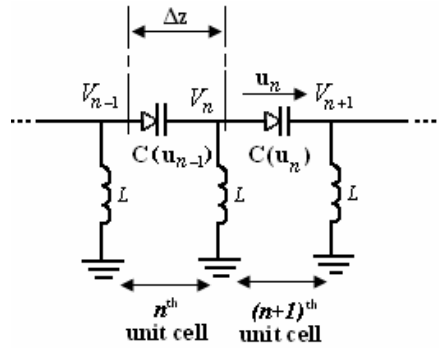


**Figure 1.** The  $n$ th and  $(n + 1)$ th unit cells of the circuit model under consideration.

First, its dispersive characteristic is anomalous; that is the lower frequency components of an excited pulse travel slower than its higher frequency components [12, 13]. Second, because of the variation of the series nonlinear capacitances by the amplitude of the wave traveling along the transmission line, the self-phase modulation (SPM) phenomenon is observed in this transmission line similar to a nonlinear optical fiber [19–21]. Because of the two effects mentioned above for the LH-NL transmission line, there is the possibility of supporting envelope soliton waves [12]. In what follows, we concentrate on deriving the governing equation of the circuit model for investigation of the soliton generation.

Applying Kirchhoff's current law (KCL) to the  $n$ th node and taking the derivative with respect to time of both sides of equations, we realize that the voltages of the adjacent nodes satisfy:

$$\frac{\partial^2 Q(V_{n-1} - V_n)}{\partial t^2} - \frac{\partial^2 Q(V_n - V_{n+1})}{\partial t^2} = \frac{1}{L} V_n, \quad (1)$$

where  $Q$  is the stored charge in the nonlinear capacitance. Next, if the nonlinear capacitance characteristic is estimated by the second-order approximation of the voltage across the capacitor ( $u$ ),  $Q$  is approximately given by:

$$Q(u) \approx C_0 u (1 + \alpha u + \beta u^2), \quad (2)$$

where  $\alpha$  and  $\beta$  are, respectively, the first- and the second-order nonlinearity coefficients of the varactors. By substituting Eq. (2) into Eq. (1) and introducing the spatial variable  $z$ , Eq. (1) leads to

$$C_0 \frac{\partial^2}{\partial t^2} \{V(z - \Delta z, t) - 2V(z, t) + V(z + \Delta z, t)\}$$

$$+ \alpha [(V(z - \Delta z, t) - V(z, t))^2 - (V(z, t) - V(z + \Delta z, t))^2] \\ + \beta [(V(z - \Delta z, t) - V(z, t))^3 - (V(z, t) - V(z + \Delta z, t))^3] \} = \frac{1}{L} V(z, t) \quad (3)$$

Here,  $V_n(t)$  is replaced by  $V(z = n \Delta z, t)$ . Now, by making the assumption that the unit cell size ( $\Delta z$ ) is very small compared to the wavelength, the Taylor expansions of  $V(z - \Delta z, t)$  and  $V(z + \Delta z, t)$  up to the third-order can be retained. Substituting the Taylor expansion into Eq. (3) yields:

$$C_0 \frac{\partial^2}{\partial t^2} \left( \Delta z^2 \frac{\partial^2 V(z)}{\partial z^2} - \alpha \Delta z^3 \frac{\partial}{\partial z} \left( \frac{\partial V(z)}{\partial z} \right)^2 \right. \\ \left. + \beta \Delta z^4 \frac{\partial}{\partial z} \left( \frac{\partial V(z)}{\partial z} \right)^3 \right) - \frac{1}{L} V(z) = 0. \quad (4)$$

By introducing the normalized variables  $T$  and  $Z$  according to:

$$T = \frac{t}{\sqrt{LC_0}} \quad Z = \frac{z}{\Delta z}. \quad (5)$$

Eq. (4) can be transformed into:

$$\frac{\partial^4}{\partial T^2 \partial Z^2} (U - \alpha U^2 + \beta U^3) - U = 0, \quad (6)$$

where

$$U = \frac{\partial V}{\partial Z}. \quad (7)$$

### 3. ASYMPTOTIC BEHAVIOR OF THE LH-NL TRANSMISSION LINE

The reductive perturbation method is used for studying the asymptotic behavior of nonlinear dispersive waves [15] and [22–24]. In this work, under the assumption of weak nonlinearity, the reductive perturbation method is applied to Eq. (6). To begin this procedure, the variables  $\xi$  and  $\tau$  are introduced as follows:

$$\xi = \varepsilon (Z - V_g T) \\ \tau = \varepsilon^2 T. \quad (8)$$

Note that  $\varepsilon$  is a small parameter and  $V_g$  denotes the group velocity of the envelope wave. The derivatives with respect to the introduced variables are given by:

$$\frac{\partial}{\partial T} \rightarrow \frac{\partial}{\partial T} - \varepsilon V_g \frac{\partial}{\partial \xi} + \varepsilon^2 \frac{\partial}{\partial \tau} \\ \frac{\partial}{\partial Z} \rightarrow \frac{\partial}{\partial Z} + \varepsilon \frac{\partial}{\partial \xi} \quad (9)$$

Now, the function  $U$  can be expanded to a power series of  $\varepsilon$  as follows:

$$U = \sum_{n=1}^{\infty} \varepsilon^n \sum_{\ell=-\infty}^{\infty} U_{\ell}^n(\xi, \tau) e^{j\ell\theta}, \quad (10)$$

where,  $\theta = kZ - \omega T$  and  $\ell$  refers to a higher-harmonic wave component. For  $U$  to be a real function, it is necessary to have  $U_{\ell}^{(1)} = U_{-\ell}^{(1)*}$ . The expression of  $U$  is substituted into the nonlinear Eq. (6) and the coefficients of each order of  $\varepsilon$  are separated and set to zero. Therefore, we obtain first-, second- and third-order sets of equations. The linear dispersion relation for  $\ell = \pm 1$  of the first-order is given by:

$$\omega^2 = \frac{1}{k^2}, \quad (11)$$

where  $\omega$  is normalized by  $1/\sqrt{LC_0}$ . Since the wave number is negative in a LH transmission line, the group velocity is given by:

$$V_g = \frac{\partial \omega}{\partial k} = \frac{1}{k^2}. \quad (12)$$

On the other hand, the third-order of  $\varepsilon$  for  $\ell = 1$  is obtained according to the following equation:

$$\begin{aligned} j \frac{\partial U_1^{(1)}}{\partial \tau} - \left( \frac{\omega^2 + 4\lambda\omega k + V_g^2 k^2}{2\omega k^2} \right) \frac{\partial^2 U_1^{(1)}}{\partial \xi^2} \\ + \frac{1}{2\omega k^2} \left( -2 \frac{16(\alpha k^2 \omega^2)^2}{16\omega^2 k^2 - 1} + 3\beta k^2 \omega^2 \right) |U_1^{(1)}|^2 U_1^{(1)} = 0. \end{aligned} \quad (13)$$

By comparing Eq. (13) with the NLS equation, that is:

$$j \frac{\partial U}{\partial \tau} + P \frac{\partial^2 U}{\partial \xi^2} + Q |U|^2 U = 0, \quad (14)$$

we have realized that  $U_1^{(1)}$  satisfies a NLS equation with the following coefficients:

$$P = \frac{1}{2} \frac{\partial^2 \omega}{\partial k^2} = \omega^3 \quad Q = \frac{\omega}{2} \left( -\frac{32}{15} \alpha^2 + 3\beta \right). \quad (15)$$

It is observed from Eq. (15) that the sign of the dispersion coefficient ( $P$ ) is always positive. But the sign of the nonlinearity coefficient ( $Q$ ) depends on the nonlinear characteristics of the capacitance. Therefore, the sign of the product  $PQ$  can be positive or negative, which leads to dark soliton ( $PQ < 0$ ) or bright soliton ( $PQ > 0$ ) generations. Thus,

by supposing that the first power of  $\varepsilon$  is dominant, the dark soliton is given by [25]:

$$U(z = n\Delta z, t) = A_0 \left[ 1 - B^2 \operatorname{sech}^2 \left\{ \left| \frac{Q}{8P} \right|^{1/2} B A_0 \left( n - V_g \frac{t}{\sqrt{LC_0}} \right) \right\} \right]^{1/2} \cos \left( kn - \frac{\omega t}{\sqrt{LC_0}} - \theta(z = n\Delta z, t) \right), \quad (16)$$

where  $A_0$  (the soliton amplitude) and  $\theta(z = n\Delta z, t)$  are:

$$\begin{aligned} A_0 &= 2\varepsilon A \\ \theta(z = n\Delta z, t) &= \left| \frac{Q}{8P} \right|^{1/2} A_0 \sqrt{1 - B^2} \left( n - V_g \frac{t}{\sqrt{LC_0}} \right) + \frac{Q}{8} (3 - B^2) A_0^2 \frac{t}{\sqrt{LC_0}} \\ &\quad + \tan^{-1} \left\{ \frac{B}{\sqrt{1 - B^2}} \tanh \left( \left| \frac{Q}{8P} \right|^{1/2} B A_0 \left( n - V_g \frac{t}{\sqrt{LC_0}} \right) \right) \right\} \end{aligned} \quad (17)$$

$B$  controls the depth of the dip soliton. The mathematical relation for the bright soliton is presented in [24].

Note that if the dissipation of the LH-NL transmission line is taken into account,  $P$  and  $Q$  coefficients obtained from the reductive perturbation method will be complex numbers. Therefore, the formed soliton is dissipated along the transmission line.

## 4. RESULTS AND SIMULATION

In order to verify our analytical prediction based on Eq. (16), we have also analyzed the electric circuit of Fig. 1 using well-known methods of circuit analysis. To this end, the circuit of Fig. 1 is connected to a source with 50 Ohms resistance and a load with 50 Ohms resistance. The number of cells between the source and the load are assumed to be 500. The circuit is then analyzed using a timedomain technique for nonlinear circuits. The method uses finite-difference applied to the differential equations governing the voltages and current of the circuit.

### 4.1. Dark Soliton

Firstly, we consider the LH-NL transmission line with a linear shunt inductance 2.5 nH and a varactor characterized by  $C(u) = 1 \text{ pF}(1 + 3\beta u^2)$ , with  $\beta = -0.1$ . In this case, the sign of the product  $PQ$  is negative. Therefore, if this circuit is excited by a dark initial signal [24],

a dark soliton will be generated. A sample input pulse having narrow dip is given by:

$$V_{in} = A_0 \tanh\left(\frac{t - \tau_0}{T_0}\right) \cos(2\pi ft), \quad (18)$$

where  $A_0 = 0.75$ ,  $T_0 = 1$  ns,  $\tau_0 = 30$  ns and  $f = 2.7$  GHz. The selected frequency is set in passband of the transmission line. The envelope waveform obtained from the finite-difference method at different positions  $z/L_0$  depicted in Fig. 2, where  $L_0$  is length of the LH-NL transmission line.

As observed in Fig. 2, the invariant dark soliton with an amplitude of  $A_0 = 0.5$  volts forms along the transmission line. Note that the dip of the pulse retains its shape.

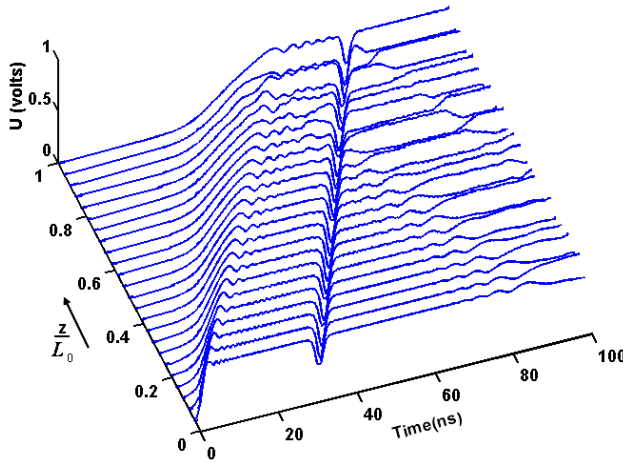


**Figure 2.** Dark soliton at different positions  $z/L_0$  obtained from simulation of the LH-NL transmission line.

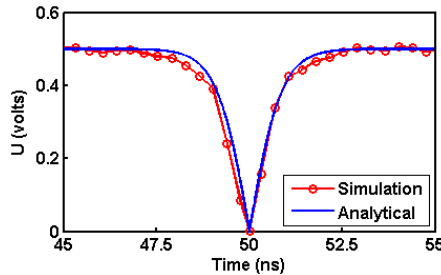


**Figure 3.** Comparison between the envelope waveform obtained from the analytical solution and the simulation.

Figure 3 compares the analytical solution of Eq. (16) and the simulation result. As observed in Fig. 3, good agreement between the analytical and simulated results. To verify that the dark soliton is caused by the nonlinearity of the LH transmission line, we have repeated the simulation with  $\beta = 0$  which corresponds to linear capacitors. Application of the waveform of Eq. (18) to this case results in the propagation shown in Fig. 4. As expected, the width of the dip broadens along the transmission line because of the LH transmission line dispersive characteristic, so no soliton waves will be observed.

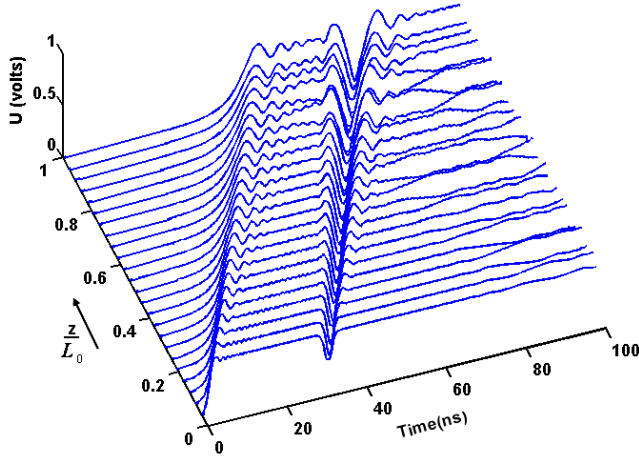


**Figure 4.** Tangent hyperbolic excitation at different positions  $z/L_0$  obtained from simulation of the LH transmission line.

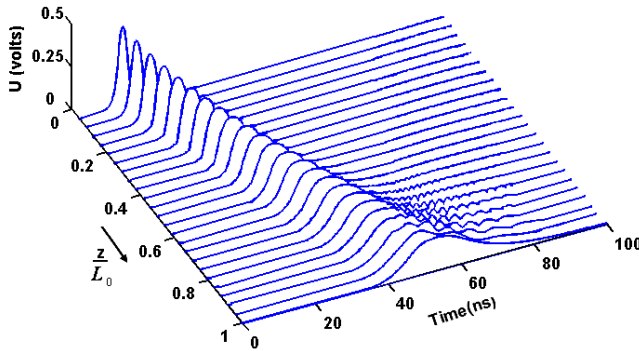


**Figure 5.** A secant hyperbolic excitation at different positions  $z/L_0$  obtained from simulation of the LH-NL transmission line.

According to the analytical calculations, this circuit because of its negative nonlinearity cannot support bright solutions. To verify this, the circuit is excited by a secant hyperbolic (i.e., a bright soliton) given by:

$$V_{in} = A_0 \operatorname{sech}\left(\frac{t - \tau_0}{T_0}\right) \cos(2\pi ft), \quad (19)$$

where  $A_0 = 0.75$ ,  $T_0 = 1$  ns,  $\tau_0 = 10$  ns and  $f = 2.7$  GHz. Propagation of this pulse along the transmission line is simulated and the obtained results are illustrated in Fig. 5. As expected, the pulse broadens while propagating along the transmission line, so soliton waves are not generated.

#### 4.2. Bright Soliton

Now, we assume a nonlinear characteristic for the varactor as  $C(u) = 1 \text{ pF}(1 + 3\beta u^2)$ , with  $\beta = 0.1$ . In this case, the circuit is excited by the pulse given by Eq. (19). Because of the positive sign of the product  $PQ$ , as predicted by the analytical solution, a bright soliton with an amplitude of  $A_0 = 0.47$  volts will be formed along the transmission line. The envelope waveforms obtained from simulation are shown in Fig. 6. As seen in this figure, the envelope waveform preserves its shape along the propagation path. Fig. 7 compares the analytical solution and the simulation results. From the results shown in Fig. 7, it is observed the analytical solution is in good agreement with the simulation result. To confirm that the bright soliton is formed due to the nonlinearity of the

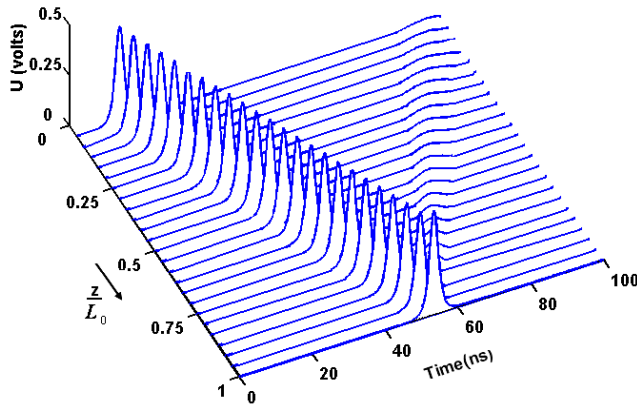


**Figure 6.** Bright soliton at different positions  $z/L_0$  obtained from simulation of the LH-NL transmission line.

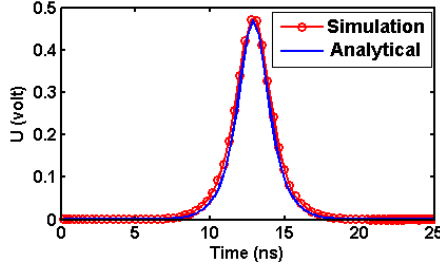


**Figure 7.** Comparison between the envelope waveform obtained by the analytical solution and the simulation.

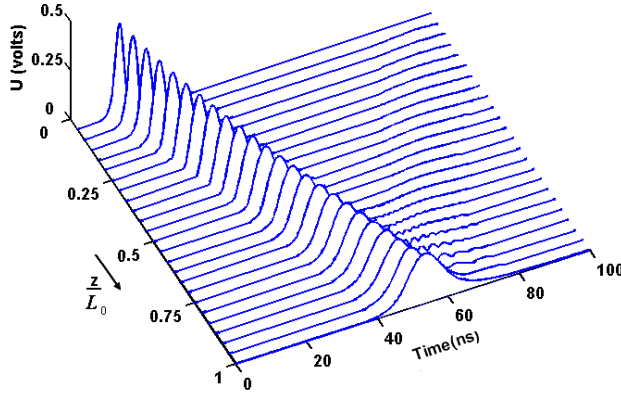


**Figure 8.** A secant hyperbolic excitation at different positions  $z/L_0$  obtained from simulation of the LH transmission line.

LH transmission line, the simulation of this circuit with  $\beta = 0$  and application of the waveform of Eq. (19) is carried out. Fig. 8 shows the simulation results at different positions  $z/L_0$ . As predicted, the width of the pulse broadens along the transmission line.

## 5. CONCLUSION

In this paper, modeling of a LH-NL transmission line loaded periodically with nonlinear *series* capacitors and linear shunt inductors is presented. The reductive perturbation method is applied to reformulate the obtained equation. It is shown that the spatial derivative of the voltage across the transmission line satisfies a NLS equation. The coefficients of the obtained NLS equation show that the dispersion coefficient ( $P$ ) is always positive, but the sign of the nonlinearity coefficient ( $Q$ ) is determined by the characteristics of the

varactor. Depending on the sign of the product  $PQ$ , the proposed LH-NL transmission line can generate either bright or dark solitons. We have verified generation of both kinds of solitons using a circuit simulator based on a finite-difference method. A good agreement is observed between the analytical prediction and the simulation results.

## ACKNOWLEDGMENT

The authors would like to thank the Iran Telecommunication Research Center (ITRC) for the financial support of this project.

## REFERENCES

1. Eleftheriades, G. V. and K. G. Balmain, *Negative-refraction Metamaterials; Fundamental Principles and Applications*, Wiley Interscience, New York, 2005.
2. Caloz, C., *Electromagnetic Metamaterials: Transmission Line Theory and Microwave Applications*, Wiley Interscience, New York, 2006.
3. Ran, L.-X., J. T. Huangfu, H. Chen, X.-M. Zhang, K.-S. Cheng, T. M. Grzegorzczuk, and J. A. Kong, "Experimental study on several left-handed metamaterials," *Progress In Electromagnetics Research*, PIER 51, 249–279, 2005.
4. Wang, J., S. Qu, J. Zhang, H. Ma, Y. Yang, C. Gu, X. Wu, and Z. Xu, "A tunable left-handed metamaterial based on modified broadside-coupled split-ring resonators," *Progress In Electromagnetics Research Letters*, Vol. 6, 35–45, 2009.
5. He, J., B.-Z. Wang, and K.-H. Zhang, "Wideband differential phase shifter using modified composite right/left handed transmission line," *Journal of Electromagnetic Waves and Applications*, Vol. 22, No. 10, 1389–1394, 2008.
6. Wang, W., C. Liu, L. Yan, and K. Huang, "A novel power divider based on dual-composite right/left handed transmission line," *Journal of Electromagnetic Waves and Applications*, Vol. 23, Nos. 8–9, 1173–1180, 2009.
7. Veselago, V. G., "The electrodynamics of substances with simultaneously negative values of  $\varepsilon$  and  $\mu$ ," *Sov. Phys. Usp.*, Vol. 10, 509–514, February 1968.
8. Tang, W. X., H. Zhao, X. Zhou, J. Y. Chin, and T.-J. Cui, "Negative index material composed of meander line and srss," *Progress In Electromagnetics Research B*, Vol. 8, 103–114, 2008.

9. Smith, D., W. Padilla, D. Vier, S. Nemat-Nasser, and S. Schultz, "Composite medium with simultaneously negative permeability and permittivity," *Phys. Rev. Lett.*, Vol. 84, 4184, 2000.
10. Caloz, C., H. Okabe, T. Iwai, and T. Itoh, "Transmission line approach of left-handed (LH) materials," *USNC/URSI Nat. Radio Science Meeting*, Vol. 1, June 2002.
11. Eleftheriades, G. V., A. K. Iyer, and P. C. Kremer, "Planar negative refractive index media using periodically L-C loaded transmission lines," *IEEE Trans. on Micr. Theory and Tech.*, Vol. 50, No. 12, 2702–2712, December 2002.
12. Caloz, C., I.-H. Lin, and T. Itoh, "Characteristics and potential applications of nonlinear left-handed transmission line," *Microw. and Opt. Tech. Lett.*, Vol. 40, No. 6, 471–473, March 2004.
13. Gupta, S. and C. Caloz, "Dark and bright solitons in left-handed nonlinear transmission line metamaterials," *IEEE MTT-S Int. Micro. Symp.*, 979–982, 2007.
14. Narahara, K., T. Nakamichi, T. Suemitsu, T. Otsuji, and E. Sano, "Development of solitons in composite right- and left-handed transmission lines periodically loaded with schottky varactors," *Journal of Appl. Phys.*, Vol. 102, 024501–024504, 2007.
15. Taniuti, T. and N. Yajima, "Perturbation method for a nonlinear wave modulation, II," *J. Math. Phys.*, Vol. 10, 2020–2024, 1968.
16. Alexander, B. K. and D. W. Van Der Weide, "Trains of envelope solitons in nonlinear left-handed transmission line media," *Appl. Phys. Lett.*, Vol. 91, 254111–254113, 2007.
17. Kozyrev, A. B. and D. W. Van Der Weide, "Nonlinear left-handed transmission line metamaterials," *J. Phys. D: Appl. Phys.*, Vol. 41, 173001–173010, August 2008.
18. Arévalo, E., "Solitons in anharmonic chains with negative group velocity," *Physical Review E*, Vol. 76, 066602–066605, December 2007.
19. Agarwal, G. P., *Nonlinear Fiber Optics*, Academic Press, 2005.
20. Gangwar, R., S. P. Singh, and N. Singh, "Soliton based optical communication," *Progress In Electromagnetics Research*, PIER 74, 157–166, 2007.
21. Biswas, A., D. Milovic, F. Majid, and R. Kohl, "Optical soliton cooling in a saturable law media," *Journal of Electromagnetic Waves and Applications*, Vol. 22, No. 13, 1735–1746, 2008.
22. Nejoh, Y., "Envelope soliton of the electron plasma wave in a nonlinear transmission line," *Physica Scripta*, Vol. 31, 415–418, 1985.

23. Nejoh, Y., "Cusp solitons, shock waves and envelope solitons in a new non-linear transmission line," *J. Phys. A: Math. Gen.*, Vol. 20, 1733–1741, 1987.
24. Marquie, P., J. M. Bilbault, and M. Remoissenet, "Generation of envelope and hole solitons in a experimental transmission line," *Phys. Rev.*, Vol. 49, No. 1, 828–835, January 1994.
25. Hasegawa, A. and M. Matsumoto, *Optical Solitons in Fibers*, 3rd edition, Springer, 2003.